

SCIENTIFIC REPORTS



OPEN

Bacterial Pore-Forming Toxins Promote the Activation of Caspases in Parallel to Necroptosis to Enhance Alarmin Release and Inflammation During Pneumonia

Norberto Gonzalez-Juarbe¹, Kelley M. Bradley¹, Ashleigh N. Riegler¹, Luis F. Reyes², Terry Brissac¹, Sang-Sang Park¹, Marcos I. Restrepo² & Carlos J. Orihuela¹

Pore-forming toxins are the most common virulence factor in pathogenic bacteria. They lead to membrane permeabilization and cell death. Herein, we show that respiratory epithelial cells (REC) undergoing bacterial pore-forming toxin (PFT)-induced necroptosis simultaneously experienced caspase activation independently of RIPK3. MLKL deficient REC treated with a pan-caspase inhibitor were protected in an additive manner against PFT-induced death. Subsequently, cleaved versions of caspases-2, -4 and -10 were detected within REC undergoing necroptosis by immunoblots and monoclonal antibody staining. Caspase activation was observed in lung samples from mice and non-human primates experiencing Gram-negative and Gram-positive bacterial pneumonia, respectively. During apoptosis, caspase activation normally leads to cell shrinkage, nuclear condensation, and immunoquiescent death. In contrast, caspase activity during PFT-induced necroptosis increased the release of alarmins to the extracellular milieu. Caspase-mediated alarmin release was found sufficient to activate resting macrophages, leading to Interleukin-6 production. In a mouse model of Gram-negative pneumonia, deletion of caspases -2 and -11, the mouse orthologue of caspase-4, reduced pulmonary inflammation, immune cell infiltration and lung damage. Thus, our study describes a previously unrecognized role for caspase activation in parallel to necroptosis, and indicates that their activity plays a critical pro-inflammatory role during bacterial pneumonia.

According to the World Health Organization, pneumonia is the leading cause of infectious death worldwide¹. Bacterial pathogens are at fault for approximately 150 million cases of pneumonia per year². Pore-forming toxins (PFTs) have a nearly ubiquitous presence in bacterial pathogens and are often responsible for a large part of the tissue injury that occurs during infection³⁻⁵. To date, PFTs have been shown to cause apoptosis, necroptosis, and pyroptosis in a variety of *in vitro* and *in vivo* models⁶. Nonetheless, the molecular mechanisms of these ubiquitous toxins during disease and their effect on the host response continues to be elucidated today.

PFTs are virulence determinants by which bacteria mediate release of sequestered nutrients from host cells, kill or incapacitate immune cells to avoid clearance, or cause inflammation that promotes dispersal⁷. PFTs have been implicated in the activation of various modes of cell death. At high doses, PFTs mediate irreversible plasma membrane permeability leading to necrotic death, mainly due to loss of osmotic regulation and/or a metabolic catastrophe⁸. At sub lytic concentrations, PFTs have been shown to cause programmed cell death including apoptosis, pyroptosis, or necroptosis⁵. Apoptosis is an immunoquiescent cell death program regulated by cysteine-aspartic proteases, called caspases. Apoptotic caspase activation can be due to intrinsic signals, such as the release of cytochrome C from damaged mitochondria^{9,10}, or extrinsic signals, including engagement of a death receptor on the cell membrane by its cognate ligand¹¹. For example, *Helicobacter pylori* vacuolating toxin vacA

¹Department of Microbiology, The University of Alabama at Birmingham, 845 19th Street South, Birmingham, Alabama, 35294-2170, USA. ²Division of Pulmonology, South Texas Veterans Health Care System, San Antonio, Texas, 78229, USA. Correspondence and requests for materials should be addressed to N.G.-J. (email: norberto@uab.edu) or C.J.O. (email: corihuel@uab.edu)

can induce apoptosis through its permeabilization of the mitochondrial inner membrane, causing a metabolic breakdown in the cell and the release of cytochrome C, leading to the activation of caspase-9¹². Alternatively, exposure to Fas ligand, triggers apoptosis through caspase-8 mediated extrinsic apoptosis¹³. Pertinent to this manuscript, apoptosis can also be initiated by less studied caspases such as caspase-2, the most evolutionarily conserved caspase, and caspase-10 upon contact with bacterial pathogens^{11,14}. How this occurs is still unclear. PFTs have also been shown to induce programmed modes of necrotic death, specifically pyroptosis and necroptosis⁷. Pyroptosis is mediated by the activation of the canonical caspase-1 or the non-canonical caspase-4^{15,16}. Caspase-4 and its murine orthologue, caspase-11, have been shown to mediate epithelial defenses against enteric bacterial pathogens by activating the inflammasome¹⁶. To date, the complete functions of caspases -2, -4, and 10 remain undefined^{10,11,17,18}.

Necroptosis, a form of programmed necrosis, is highly inflammatory due to the purposeful release of cytosolic molecules containing danger-associate-molecular-patterns, i.e. alarmins. Necroptosis is modulated by receptor-interacting serine-threonine kinases -1 and -3 (RIPK1, RIPK3) and occurs when caspase-8, a pivotal apoptotic caspase, is inhibited. Briefly, caspase-8 inactivates both RIPK1 and RIPK3 by sequestration or proteolytic cleavage^{19,20}. When cellular distress signals are present and caspase-8 is inactive, RIPK3 binds to RIPK1 forming the necroptosome. The necroptosome phosphorylates mixed lineage kinase domain-like protein (MLKL), which then integrates and damages cell membranes, leading to necrotic death^{19–21}. Importantly, necroptosis is understood and is by definition exclusive of caspase activity^{19,21}. This is supported by our own studies that showed no impact of caspase-inhibition on PFT-mediated necroptotic death of macrophages²². In addition, it has also been reported that caspase-8 activity suppresses RIPK3 activation¹⁹. Nonetheless, a recent report showed that during influenza A respiratory tract infection, caspase-8 induced apoptosis occurred in parallel to necroptosis in a RIPK3 dependent manner²³. Thus, the distinction between apoptosis and necroptosis may not be so clear cut.

In recent work, we have shown that PFTs activate the necroptosis pathway in macrophages²² and respiratory epithelial cells (REC)²⁴ and this contributes to pulmonary injury during bacterial pneumonia. PFT-induced necroptosis required RIPK1, RIPK3 and MLKL, yet was activated independently of death receptor engagement through non-canonical means, i.e. ion dysregulation as the result of membrane permeabilization²⁴. One important distinction between macrophage and REC death is that only partial protection against PFTs was observed in REC following necroptosis inhibition. In contrast, PFT-induced death in macrophages was unequivocally blocked by necroptosis inhibition. Based upon these results, we hypothesized that a second cell death signaling pathway was active in PFT-exposed REC.

Results

Pore-forming toxins promote the simultaneous activation of caspases and necroptosis during infection. Pre-treatment of A549 type II pneumocytes with the general caspase inhibitor Z-VAD-FMK (Zvad) and either RIPK1 inhibitor necrostatin-1s (Nec1s) (Fig. 1a), RIPK1 inhibitor necrostatin-5 (Nec5) (Fig. 1b), RIPK3 inhibitor GSK' 872 (Fig. 1c), or MLKL inhibitor necrosulfonamide (Fig. 1d), all protected in an additive manner versus pretreatment with each drug alone against *Serratia marcescens* (*Sma*) infection. Similar results were observed when A549 cells were pre-treated with Nec-5 and Z-VAD-FMK and challenged with recombinant pneumolysin (rPly) and a similar, very strong, trend with recombinant α -toxin (Supplementary Fig. 1); the latter two being PFTs produced by *Streptococcus pneumoniae* (*Spn*) and *Staphylococcus aureus*, respectively. Conclusively, A549 cells with MLKL deleted using CRISPR-Cas9 experienced additive protection when treated with Zvad (Fig. 1e).

Viral infections have been reported to simultaneously trigger necroptosis and RIPK3/caspase-8 mediated apoptosis within mammalian fibroblasts and lung epithelial cells²³. Following influenza challenge, RIPK3 has been shown to activate caspase-8¹⁶. To test for this, we transfected A549 cells with siRNA targeting MLKL and caspase-8 and challenged these with *Sma*. No additive protection was observed in the MLKL and caspase-8 knockdown cells (Fig. 1f, Supplementary Fig. 2). Importantly, no activation of caspases-1, -3 or -8 was observed in *Sma* challenged A549 cells; conversely this was observed when A549 cells were challenged with positive control cyclohexamide or LPS/nigericin (Supplementary Fig. 3). Simultaneous siRNA knockdown of RIPK3 and MLKL also did not have an additive protective effect following *Sma* challenge (Fig. 1f). Together, these results suggest a different form of caspase-associated cell death was occurring in PFT-exposed RECs, one independent of canonical intrinsic or extrinsic apoptosis.

At low multiplicity of infection (MOI), chemical inhibition of caspases -2, -4, -6 and -10, but not -1, -3, -8, or -9 was found to confer significant protection against *Sma* (Fig. 2a). At high infectious MOI, protection incurred by inhibition of caspase-6 was lost (Supplementary Fig. 4a). Comparable results were observed when A549 cells were challenged with rPly or α -toxin and when normal human bronchial epithelial cells (NHBEs) were challenged with *Sma* and rPly (Supplementary Fig. 4b–e). Immunoblots for phosphorylated MLKL and cleaved caspases-2, -4, and -10 showed the active version of these proteins in lysates from A549 cells infected with *Sma* (Fig. 2b). Likewise, A549 cell death was decreased after siRNA knockdown of caspases -2, -4, and -10, but not after siRNA knockdown of caspase-1 and -8 (Fig. 2c, Supplementary Fig. 5a). Again, similar results were also observed after A549 cells were challenge with rPly or α -toxin (Supplementary Fig. 5b,c). Finally, an important role for activation of caspases -2, -4, and -10 following PFT exposure, and one that was not dependent on necroptosis, was suggested after additional protection of MLKL deficient A549 cells against *Sma* when pre-treated with inhibitors of these caspases (Fig. 2d).

To verify that caspase activation and necroptosis occurred within the same cell, A549 cells were first examined using propidium iodide (PI), which enters necrotic cells, and then caspase-active specific fluorescent-labeled inhibitors of caspases (FLICA)²⁵ after challenge with rPly. We observed that both A549 and NHBEs were PI positive and pan-caspase FLICA positive, providing evidence of ongoing caspase activation and necrosis within the same cell. PI positive cells were also FLICA positive for caspase-2 and -10, but not caspase-1,

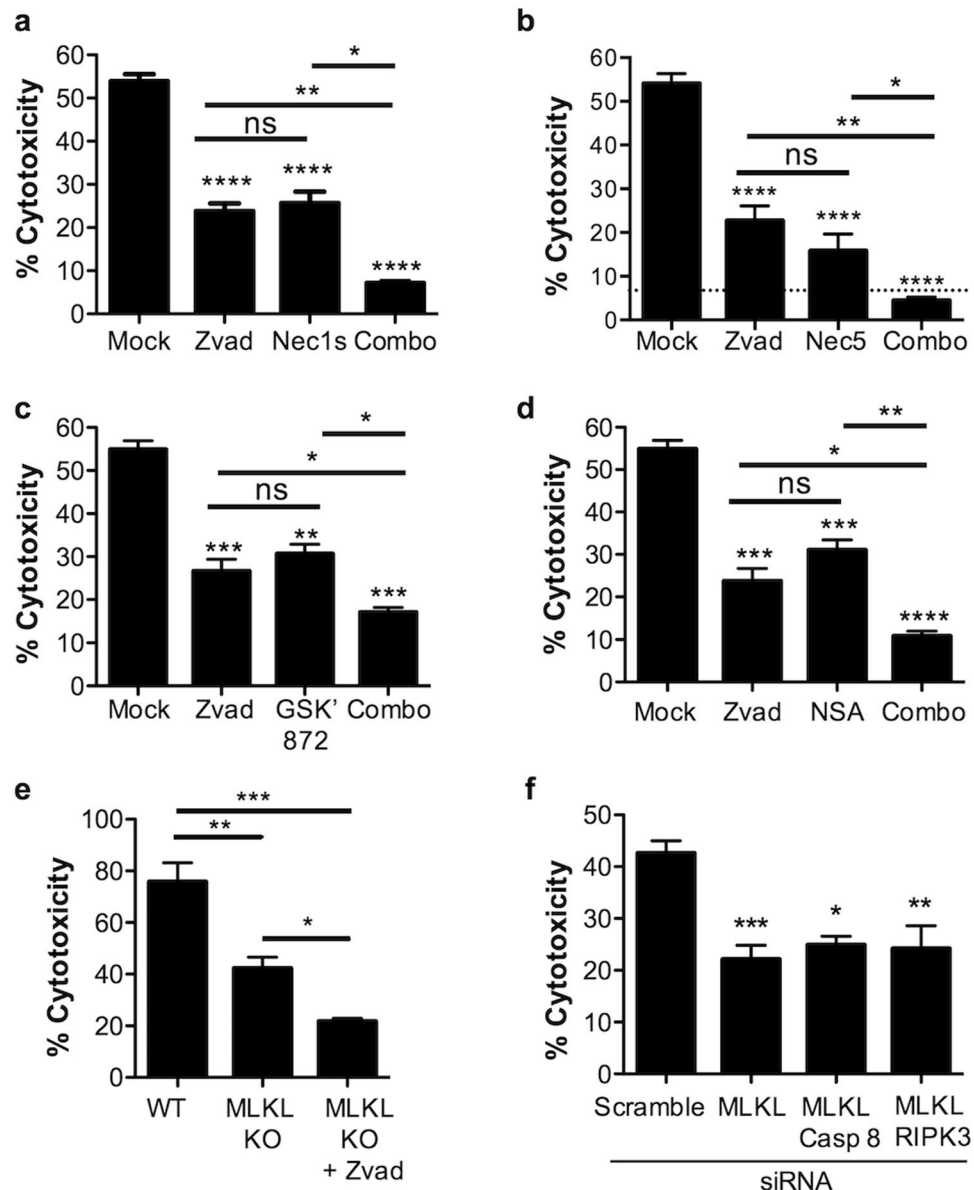


Figure 1. Pore-forming toxins promotes RIPK3-independent activation of caspases and necroptosis to induce cell death. **(a)** LDH release cytotoxicity assay of *Sma* infected A549 cells pre-treated with the pan-caspase inhibitor, Z-VAD-FMK (Zvad, 100 μ M), necrostatin-1s (Nec1s, 100 μ M), or a combination of Zvad and Nec1s (Combo, 100 μ M each). LDH release cytotoxicity assay of *Sma* infected (MOI 10) A549 cells pre-treated with the pan-caspase inhibitor, Z-VAD-FMK (Zvad, 100 μ M), **(b)** RIPK1 inhibitor necrostatin-5 (Nec5, 100 μ M), **(c)** RIPK3 inhibitor GSK' 872 (GSK' 872, 100 μ M), **(d)** MLKL inhibitor necrosulfonamide (NSA, 10 μ M) or a combination of both (Combo). **(e)** LDH release cytotoxicity assay of wild-type A549 cells or A549 cells deficient in MLKL by CRISPR-Cas9 infected with *Sma* after pretreatment with Z-VAD-FMK or Mock treated. **(f)** LDH release cytotoxicity assay of A549 cells infected with *Sma* following knockdown of MLKL, MLKL/caspase-8 or RIPK3/caspase-8 by siRNA (Blots demonstrating siRNA knock down are shown in Supplementary Figure 3). For multiple group comparisons Kruskal-Wallis test with Dunn's multiple-comparison post-test was used to test every experimental condition against the mock and between experimental conditions: * $P \leq 0.05$, ** $P \leq 0.01$, *** $P \leq 0.001$, **** $P \leq 0.0001$. For *in vitro* experiments averaged data from >3 separate experiments are shown.

or -3/7 (Supplementary Fig. 6). Because FLICA may be non-specific, we subsequently examined cells with fluorophore-labeled monoclonal antibodies against cleaved caspase-2, -3, -4, -10, and pMLKL. Consistent with prior results, we observed simultaneous caspase-2, -4 and -10 activation with necroptosis in *Sma* (Fig. 2e). This too was observed in rPly or α -toxin challenged cells (Supplementary Fig. 7).

Caspase activation during PFT-mediated death changes the morphological characteristics of necroptosis. Canonical necroptosis results in cell membrane dissolution, release of cytoplasmic components, and preservation of the nucleus¹⁹. In contrast, apoptosis involves cell shrinkage, nuclear fragmentation, and the

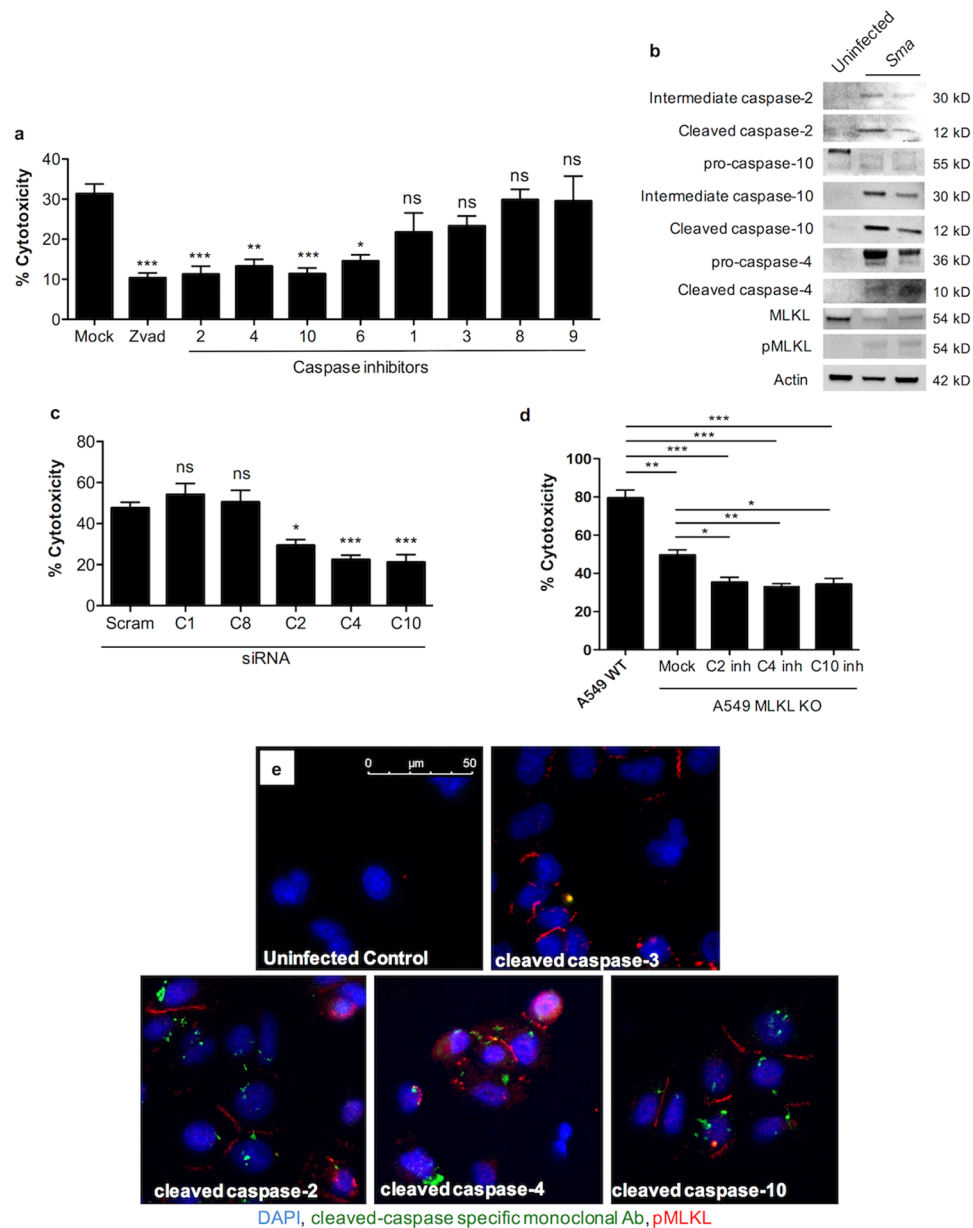


Figure 2. Caspase activity occurs in parallel to necroptosis and can be observed at the single cell level. (a) Percent cytotoxicity of *Sma* infected (MOI 0.5) A549 cells pre-treated with Zvad or inhibitors against caspases (C)-1, -2, -3, -4, -6, -8, -9, and -10 (100 μM). Mock infected cells received an equivalent amount of DMSO in media. (b) Western blots for the activation of caspase-2, caspase-10, caspase-4, MLKL and pMLKL in A549 cells infected with *Sma*. Blots images were cropped from separate gels, uninfected control (first lane) vs *Sma* infected cells (second and third lane) are shown side-by-side in the same gel. (c) LDH release cytotoxicity assay of A549 cells infected with *Sma* following knockdown of caspase-1, caspase-8, caspase-4, caspase-10 and caspase-2 by siRNA. (Blots demonstrating siRNA knock down are shown in Supplementary Figure 6a) (d) LDH release cytotoxicity assay of wild-type A549 cells or A549 cells deficient in MLKL by CRISPR-Cas9 infected with *Sma* after pretreatment with inhibitors against caspase-2(C2inh), caspases-4(C4inh) and caspases-10(C10inh) or Mock treated. (e) IF Staining for pMLKL, cleaved caspase-2, cleaved caspase-3, cleaved caspase-4 and cleaved caspase-10 in A549 cells challenged with *Sma*. Cell nucleus (DAPI, Blue), caspases (green), pMLKL (Red). For multiple group comparisons Kruskal-Wallis test with Dunn's multiple-comparison post-test was used: *P < 0.05, **P < 0.01, ***P < 0.001. For *in vitro* experiments averaged data from >3 separate experiments are shown.

formation of apoptotic bodies¹⁰. We sought to determine if caspase activity affected the morphological characteristics of cell death in A549 cells treated with pneumolysin in the presence or absence of Zvad (Fig. 3). In cells where caspase activity was not inhibited, transmission electron microscopy images showed less membrane blebbing or “bubbles” than necroptotic cells. In addition, we also observed increased mitophagy, paraptotic-like

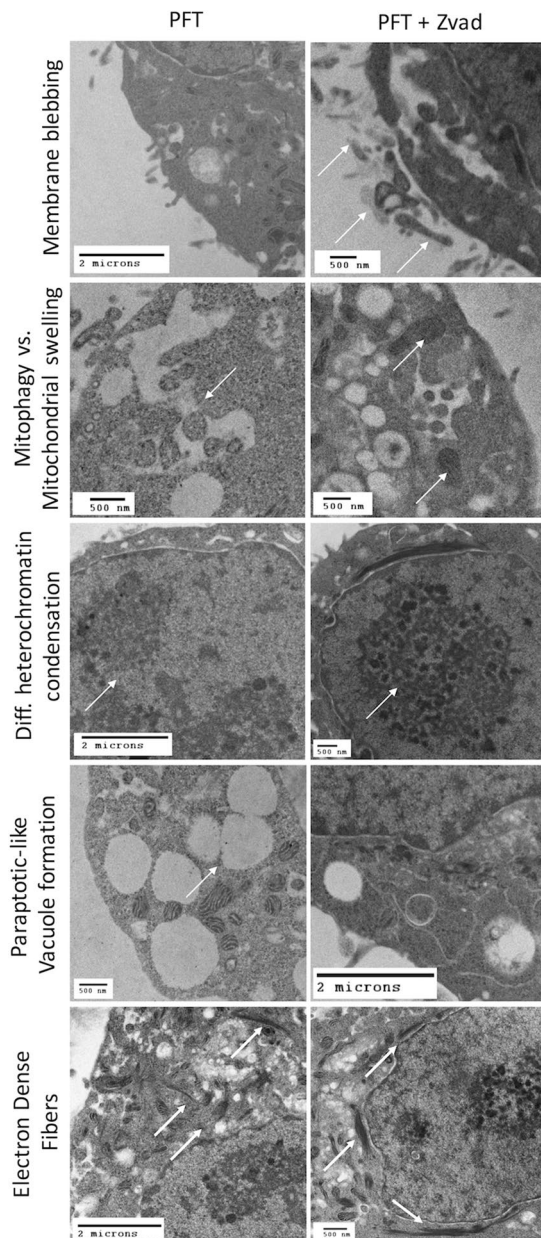


Figure 3. Caspase activity parallel to necroptosis alters PFT-mediated cell death morphology. Representative transmission electron microscopy images of rPly (rPly, 0.32 $\mu\text{g}/\text{mL}$) challenged A549 cells mock treated (for parallel caspase-necroptosis activation) or pre-treated with Z-VAD-FMK (Zvad, for necroptosis, 100 μM). Scale bars with defined dimensions are shown within each picture.

vacuolation, and heterochromatin condensation in comparison to those undergoing solely necroptosis. In contrast, Zvad treated cells solely undergoing necroptosis showed mitochondrial swelling, singular heterochromatin condensation, and perinuclear electron dense fibers. Interestingly, perinuclear localization of electron dense fibers occurred in greater magnitude in cells treated with Zvad than those with intact caspase activity.

Caspase activation parallel to necroptosis enhances alarmin release from necroptotic cells and promotes the host inflammatory response. Due to the observed differences described above, we also hypothesized that caspase activation parallel to necroptosis modulates the alarmins that are released from dying cells. To test this, we pretreated A549 cells with Zvad or the NSA, and measured levels of known alarmins released into the cell supernatants following challenge with rPly. We found that caspase activity promoted the release of S100A9 and Hsp60 into the cell supernatants (Fig. 4a). To assess the effect of caspase-mediated alarmin release on bystander immune cells, we challenged mock or Zvad treated A549 cells with rPly and collected their supernatants. Subsequently, the activity of residual rPly was neutralized with a monoclonal antibody²⁶ and the supernatants from these cells were used to challenge human macrophages (THP-1 cells). We found that IL-6 production

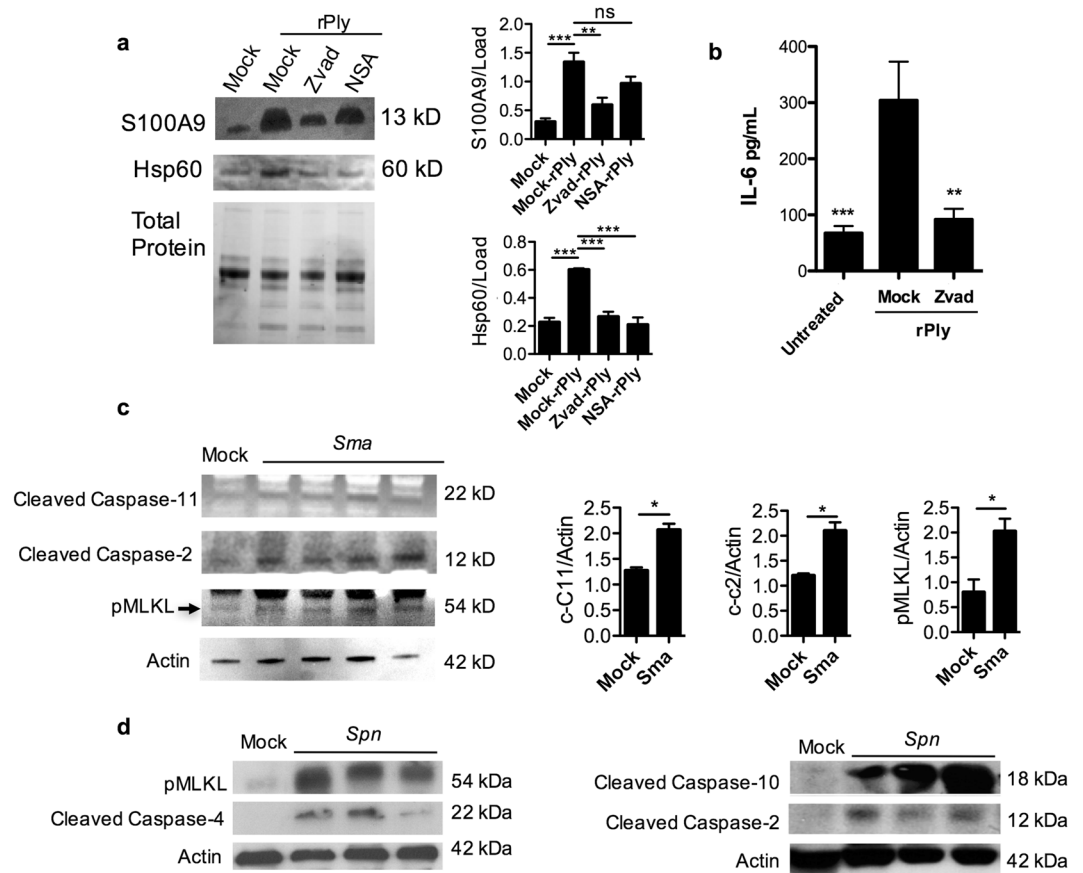


Figure 4. PFT-mediated caspase activity simultaneous to necroptosis promotes alarmin release and inflammation. **(a)** Western blots for S100A9 and HSP60 from A549 cells challenged with rPly after pre-treatment with Z-VAD-FMK (Zvad, 100 μ M), or necrosulfonamide (NSA, 10 μ M). Blots images were cropped from separate gels, uninfected control (first lane) vs rPly challenged cells (2–4 lanes) are shown side-by-side in the same gel. Densitometry from 3 separate gels is shown next to the immunoblots. **(b)** IL-6 (pg/ml) in supernatants of THP-1 macrophages challenged with the supernatants of A549 cells that were challenged with rPly (subsequently blocked by antibody) pre-treated with Z-VAD-FMK (Zvad, 100 μ M), or mock treated. **(c)** Western blot for pMLKL, cleaved caspase-2, and cleaved caspase-4 and actin (loading control) in the lungs of mice ($n = 3–4$) infected *Sma* via intratracheal route vs uninfected control. Blots images were cropped from separate gels, uninfected control (first lane) vs *Sma* infected mice (2–5 lanes) are shown side-by-side in the same gel. Densitometry from 3 separate gels is shown next to the immunoblots. Extra mock infected controls for densitometry were ran in separate gel. **(d)** Healthy baboons were challenged intrabronchially with *Spn* using a video assisted bronchoscope and sacrificed 5–7 days after infection for tissue collection. Western blot for pMLKL, cleaved caspase-2, cleaved caspase-4 and actin (loading control) in the lungs of *Spn* infected baboons vs uninfected control. Blots images were cropped from separate gels, uninfected control (first lane) vs *Spn* infected baboon's (2–4 lanes) are shown side-by-side in the same gel. For multiple group comparisons Kruskal-Wallis test with Dunn's multiple-comparison post-test was used: * $P \leq 0.05$, ** $P \leq 0.01$, *** $P \leq 0.001$. For *in vitro* experiments averaged data from >3 separate experiments are shown.

by human THP-1 macrophages was reduced when exposed to supernatants from cells that had caspase activity inhibited during PFT-induced necroptosis (Fig. 4b).

Validating this *in vivo*, we observed increased levels of cleaved caspase-2, cleaved caspase-11, and pMLKL in lung samples from mice challenged intratracheally with *Sma* (Fig. 4c, Supplementary Fig. 8a). Whereas in lung samples from non-human primates with experimental *Spn* pneumonia we also observe increased levels of cleaved caspase-2, -4 and -10 along with pMLKL (Fig. 4d, Supplementary Fig. 8b). Critically, mice deficient in caspase-2 or caspase-11 that had been challenged with *Sma* showed a stark reduction in lung consolidation when compared to wildtype, similar to mice deficient in MLKL (Fig. 5a). Immunofluorescent staining against Ly6G, a canonical marker of mature neutrophils, showed a substantial decrease in granulocyte infiltration into the lungs (Fig. 5b, Supplementary Fig. 8c) that coincided with reduced Interleukin-1 α and KC levels in lung homogenates (Fig. 5c). Thus, caspase activation worsened severity of pneumonia.

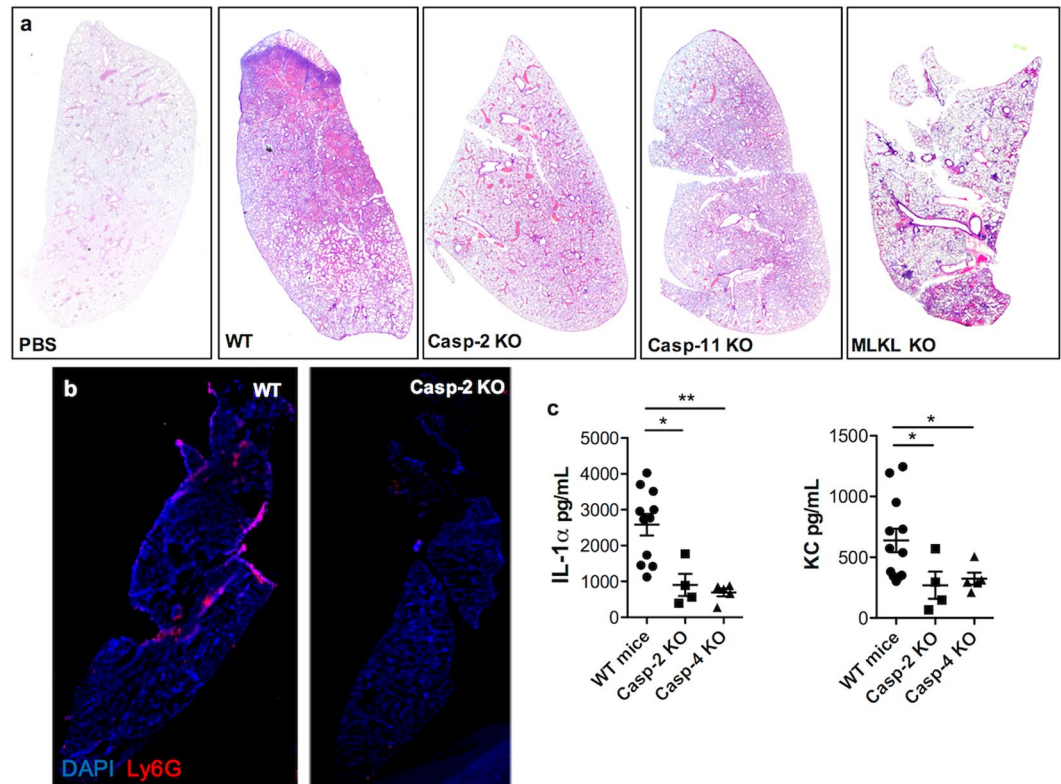


Figure 5. Caspase-2 and -11 KO reduces PFT-mediated inflammation during bacterial pneumonia. (a) Hematoxylin and Eosin stain of mice genetically deficient in MLKL, caspase-2 and caspase-4 experiencing *Sma* pneumonia or mock challenged with PBS. (b) Representative IF staining of lungs of caspase-2 KO mice infected with *Sma*, cell nucleus (DAPI, Blue), Ly6G (red). (c) Levels of IL-1 α and KC in lung homogenates from wild-type, caspase-2 KO and caspase-4 KO mice infected with *Sma*. For multiple group comparisons Kruskal-Wallis test with Dunn's multiple-comparison post-test was used: * $P \leq 0.05$, ** $P \leq 0.01$, *** $P \leq 0.001$. For *in vitro* experiments averaged data from >3 separate experiments are shown.

Discussion

REC play many critical immunological roles during bacterial infection; they serve as a physical barrier, secrete mucus and anti-microbial molecules, and produce chemokines that recruit immune cells to the site of infection^{27,28}. In the recent past we have shown that PFTs cause necroptosis of REC and this is, in large part, responsible for the pulmonary injury that occurs during pneumonia²⁴. Herein, we demonstrate that upon challenge with PFTs, RECs undergo necroptosis with parallel caspase activity and this potentiates the inflammatory response by enhancing the release of alarmins from dying cells. Our results raise questions and open new lines of investigation that can improve our understanding of basic mechanisms of infectious disease and the host response. For example, what other cell types experience parallel caspase activation to necroptosis following exposure to a PFT and why is this not the case for macrophages? Is there a PFT-mediated necroptosis-caspase signaling intersection where MLKL potentiates caspase activity, albeit these pathways seem independent? These are critical questions that now require detailed exploration.

One overriding question is that it is unknown how these caspases are being activated. Caspase-2 can function as an initiator and/or effector caspase, a capability that matches its ancient and conserved function¹⁷. Caspase-2 might, in some fashion, recognize the binding of PFTs to the plasma membrane or the associated consequences¹⁴. In this manner, caspase-2 may aggregate, oligomerize, and autoprocess itself upon PFT challenge of cells²⁹. It is important to note that caspase-2 has been shown not to process canonical apoptosis effectors such as caspases -3, -6 or -7³⁰. Instead it leads to the induction of apoptosis by increasing the release of death mediators from the mitochondria³⁰. In addition, caspase-2 has been shown to be involved in cell death mediated by cellular stress such as DNA damage, ER stress, or metabolic catastrophe³¹. A review of the literature also suggests that targeting of the mitochondria by MLKL, or even by the PFT itself, may activate mitochondrial localized caspase-2³². Other substrates released from damaged mitochondria include BID, ICAD, and PKC δ which promote mitochondrial outer membrane permeabilization activation and DNA fragmentation²⁹, and all of which are known caspase-2 substrates or initiating signals²⁹. For these reasons, we speculate that RIPK activation might further promote caspase activation upon MLKL-driven mitochondrial damage³³ although this association would not be required for necroptosis.

Our data using human cells and baboon samples show that caspase-10 is active upon PFT challenge. Caspase-10 is a homolog of caspase-8, and is highly conserved throughout multiple species, however absent in mice. Caspase-10 has been shown to have a key role in death receptor-mediated apoptosis³⁴. Importantly, it has been shown that

caspase-10 reduces death-inducing signaling complex (DISC) association and activation of caspase-8, by this it negatively regulates caspase-8 mediated death³⁵. Notably, for necroptosis to occur, caspase-8 has to be inhibited, suggesting that upon PFT challenge the activation of caspase-10 might promote necroptosis and at the same time serve as an initiator for other death mediators. In addition, caspase-10 activation through a membrane receptor could also explain the activation of caspase-2. However, the latter has yet to be elucidated.

Caspase-4 is an inflammatory caspase, recently linked to the non-canonical activation of the inflammasome and the release of IL-1 β . This is known to occur after cells are exposed to intracellular lipopolysaccharide³⁶. PFTs might be a way to introduce LPS into the cytosol during Gram-negative infections. However, we observed caspase-4 activation in cells challenged with purified PFTs (tested to be endotoxin free). One possible reason caspase-4 is activated in an LPS-independent manner may be endoplasmic reticulum stress caused by PFT-induced ion dysregulation, cellular ROS generation, and uncontrolled metabolic changes^{5,24}. Endoplasmic reticulum stress has been implicated as an activator of caspase-4 in other model systems^{37,38}. Regardless, activation of caspase-4, and presumably the inflammasome, would allow for respiratory epithelial cells to produce and release pro-inflammatory mediators during PFT-mediated necroptosis. Whether this occurs is currently being investigated.

How caspase activity acts on organelle disassembly to impact alarmin release is not clear. Yet, caspase-inhibited REC challenged with rPly had obvious differences in cellular traits during death versus controls, and released less alarmins. That caspase-activation further promoted necroptosis-driven inflammation in the airway was also unambiguous. This was evidenced *in vitro*, where naïve macrophages treated with cell supernatants from caspase inhibited REC responded less vigorously than controls, as well as *in vivo*, where we observed that caspase-2 and caspase-11 KO mice had reduced tissue damage and levels of measurable inflammatory chemokines and cytokines. The recognition that caspase activation contributes to pulmonary inflammation marks the involved caspases as potential targets for adjunct therapeutic intervention along with antimicrobials. In this instance not to clear the pathogen, but to reduce lung injury due to the excessive host response.

Herein, we have discovered that caspase activity, other than caspase-8, can occur parallel to the necroptosis machinery. Caspase activation may occur as an evolutionary conserved response to PFTs during pulmonary infections^{14,29,39,40}. In the airway, caspase activity during necroptosis was observed to exacerbate pulmonary inflammation by modulating the physical properties of cell death, which in turn impacted alarmin release. The almost universal presence of PFTs in bacterial pathogens makes this discovery highly significant and identifies caspases as potential targets for novel intervention strategies. Numerous unanswered questions remain as to how caspase activation is initiated and whether it is intertwined with necroptosis signaling. Which other cells and diseases might include a version of this form of cell death is also unknown and requires further investigation.

Methods

Ethics Statement. Animal experiments were performed using protocols approved by the Institutional Animal Care and Use Committee at the University of Alabama at Birmingham (Protocol # 20270). Animal care and protocols followed the NIH Guide for the Care and Use of Laboratory Animals.

Infections of Mice and Baboons. Female 6–8-week-old wildtype C57BL/6 mice from Jackson Laboratories (Sacramento, California) were used. MLKL knockout mice in the C57BL/6 background were obtained from Dr. Warren Alexander⁴¹. Caspase-2 KO (007899) and Caspase-11 KO (024698) mice were obtained from The Jackson Laboratory (Sacramento, California). Oropharyngeal aspiration was performed on each mouse as previously described with an inoculum of 100 μ l of a $\sim 1.0 \times 10^6$ CFU dose⁴². Briefly, after being anesthetized (2% vaporized isoflurane) each mouse was hung upright by its incisors, the tongue gently pulled outward with blunt forceps, and the respective inoculum pipetted into the pharynx accompanied by coverage of the nares to achieved forced inhalation. All mice experiments were performed with protocols approved by the University of Alabama at Birmingham Institutional Animal Care and Use Committee and in agreement with the NIH Guide for the Care and Use of Laboratory Animals. Healthy baboons, with a median age 11 (Interquartile ratio [IQR], 10–19) years old were intrabronchially challenged with *Spn* (1×10^9 CFU) using a bronchoscope^{43,44}. Between 5–7 days after infection during severe pneumonia animals were sacrificed and lung tissue was collected. All baboon experiments were performed using protocols approved by the Southwest National Primate Research Center Institutional Animal Care and Use Committee and in agreement with the NIH Guide for the Care and Use of Laboratory Animals.

Microscopy and Image Capture. Images were captured using a Zeiss AxioXam MRm Rev3 and/or MRc cameras attached to a Zeiss AxioImager Z1 epifluorescent microscope (Carl Zeiss, Thornwood, NY) or a Leica LMD6 with DFC3000G-1.3-megapixel monochrome camera (Leica Biosystems, Buffalo Grove, IL).

Inhibitors and other chemicals. RIPK1 inhibitor Necrostatin-5 was obtained from Sigma Aldrich (St. Louis, MO). Necrostatin-1s and GSK872 were obtained from BioVision (Milpitas, California). Necrosulfonamide was obtained from Tocris Bioscience (QL, United Kingdom). To inhibit caspases, we used Z-VAD-fmk, general caspase inhibitor, Z-WEHD-fmk, caspase-1 inhibitor, Z-VDVAD-fmk, caspase-2 inhibitor, Z-DEVD-fmk, caspase-3 inhibitor, Z-YVAD-fmk, caspase-4 inhibitor, Z-VEID-fmk, caspase-6 inhibitor, Z-IETD-fmk, caspase-8 inhibitor, Z-LEHD-fmk, caspase-9 inhibitor, Z-AEVD-fmk, caspase-10 inhibitor, obtained from R & D Systems (Minneapolis, MN).

Transmission electron microscopy (TEM). Published protocols were used for tissue processing⁴⁵. TEM images were obtained at the University of Alabama at Birmingham electron microscopy core, using FEI-Tecnai T12 Spirit 20–120kv, equipped with an AMT digital camera.

Silencing RNA and CRISPR-Cas9. Commercially available siRNA targeting RIPK1, RIPK3, MLKL, caspase-1, caspase-2, caspase-4, caspase-8 and caspase-10 (Santa Cruz, Dallas, TX) were used to transfect A549 alveolar epithelial cells following the manufacturer instructions. Commercially available CRISPR-Cas9 plasmids to knock out MLKL (Santa Cruz, Dallas, TX) were used following the manufacturer instructions.

Statistical analysis. Prism 7 (Graph Pad Software, La Jolla CA) was used for graph development and statistical analysis. Mann-Whitney U tests were applied for two-group comparisons, and nonparametric Kruskal-Wallis test and Dunn's *post hoc* analysis were used for multiple-group comparisons.

Data availability. The data generated in the current study are available from the corresponding author on reasonable request.

References

1. WHO. Pneumonia Fact Sheet. (2016).
2. Ruuskanen, O., Lahti, E., Jennings, L. C. & Murdoch, D. R. Viral pneumonia. *The Lancet* **377**, 1264–1275 (2011).
3. Alouf, J. E. Molecular features of the cytolytic pore-forming bacterial protein toxins. *Folia microbiologica* **48**, 5–16 (2003).
4. Gonzalez, M. R., Bischofberger, M., Pernot, L., van der Goot, F. G. & Freche, B. Bacterial pore-forming toxins: the (w)hole story? *Cellular and molecular life sciences: CMLS* **65**, 493–507, <https://doi.org/10.1007/s00018-007-7434-y> (2008).
5. Los, F. C., Randis, T. M., Aroian, R. V. & Ratner, A. J. Role of pore-forming toxins in bacterial infectious diseases. *Microbiology and molecular biology reviews: MMBR* **77**, 173–207, <https://doi.org/10.1128/MMBR.00052-12> (2013).
6. Dal Peraro, M. & Van Der Goot, F. G. Pore-forming toxins: ancient, but never really out of fashion. *Nature Reviews Microbiology* **14**, 77–92 (2016).
7. Bischofberger, M., Gonzalez, M. R. & van der Goot, F. G. Membrane injury by pore-forming proteins. *Current opinion in cell biology* **21**, 589–595 (2009).
8. Knapp, O. *et al.* Clostridium septicum alpha-toxin forms pores and induces rapid cell necrosis. *Toxicon: official journal of the International Society on Toxinology* **55**, 61–72, <https://doi.org/10.1016/j.toxicon.2009.06.037> (2010).
9. Acehan, D. *et al.* Three-dimensional structure of the apoptosome: implications for assembly, procaspase-9 binding, and activation. *Mol Cell* **9**, 423–432 (2002).
10. Elmore, S. Apoptosis: a review of programmed cell death. *Toxicol Pathol* **35**, 495–516, <https://doi.org/10.1080/01926230701320337> (2007).
11. McIlwain, D. R., Berger, T. & Mak, T. W. Caspase functions in cell death and disease. *Cold Spring Harb Perspect Biol* **5**, a008656, <https://doi.org/10.1101/cshperspect.a008656> (2013).
12. Rasso, J. Helicobacter pylori vacuolating toxin A and apoptosis. *Cell Commun Signal* **9**, 26, <https://doi.org/10.1186/1478-811X-9-26> (2011).
13. Nagata, S. Fas ligand-induced apoptosis. *Annu Rev Genet* **33**, 29–55, <https://doi.org/10.1146/annurev.genet.33.1.29> (1999).
14. Imre, G. *et al.* Caspase-2 is an initiator caspase responsible for pore-forming toxin-mediated apoptosis. *The EMBO journal* **31**, 2615–2628 (2012).
15. Fink, S. L. & Cookson, B. T. Caspase-1-dependent pore formation during pyroptosis leads to osmotic lysis of infected host macrophages. *Cell Microbiol* **8**, 1812–1825, <https://doi.org/10.1111/j.1462-5822.2006.00751.x> (2006).
16. Knodler, L. A. *et al.* Noncanonical inflammasome activation of caspase-4/caspase-11 mediates epithelial defenses against enteric bacterial pathogens. *Cell Host Microbe* **16**, 249–256, <https://doi.org/10.1016/j.chom.2014.07.002> (2014).
17. Fan, T. J., Han, L. H., Cong, R. S. & Liang, J. Caspase family proteases and apoptosis. *Acta Biochim Biophys Sin (Shanghai)* **37**, 719–727 (2005).
18. Galluzzi, L., Lopez-Soto, A., Kumar, S. & Kroemer, G. Caspases Connect Cell-Death Signaling to Organismal Homeostasis. *Immunity* **44**, 221–231, <https://doi.org/10.1016/j.immuni.2016.01.020> (2016).
19. Newton, K. & Manning, G. Necroptosis and Inflammation. *Annual review of biochemistry* **85**, 743–763, <https://doi.org/10.1146/annurev-biochem-060815-014830> (2016).
20. Pasparakis, M. & Vandenabeele, P. Necroptosis and its role in inflammation. *Nature* **517**, 311–320 (2015).
21. Hildebrand, J. M. *et al.* Activation of the pseudokinase MLKL unleashes the four-helix bundle domain to induce membrane localization and necroptotic cell death. *Proceedings of the National Academy of Sciences* **111**, 15072–15077 (2014).
22. Gonzalez-Juarbe, N. *et al.* Pore-Forming Toxins Induce Macrophage Necroptosis during Acute Bacterial Pneumonia. *PLoS pathogens* **11**, e1005337, <https://doi.org/10.1371/journal.ppat.1005337> (2015).
23. Nogusa, S. *et al.* RIPK3 Activates Parallel Pathways of MLKL-Driven Necroptosis and FADD-Mediated Apoptosis to Protect against Influenza A Virus. *Cell Host Microbe* **20**, 13–24, <https://doi.org/10.1016/j.chom.2016.05.011> (2016).
24. Gonzalez-Juarbe, N. *et al.* Pore-forming toxin-mediated ion dysregulation leads to death receptor-independent necroptosis of lung epithelial cells during bacterial pneumonia. *Cell Death Differ*, <https://doi.org/10.1038/cdd.2017.49> (2017).
25. Smolewski, P., Grabarek, J., Halicka, H. D. & Darzynkiewicz, Z. Assay of caspase activation *in situ* combined with probing plasma membrane integrity to detect three distinct stages of apoptosis. *J Immunol Methods* **265**, 111–121 (2002).
26. de los Toyos, J. R. *et al.* Functional analysis of pneumolysin by use of monoclonal antibodies. *Infection and immunity* **64**, 480–484 (1996).
27. Chuquimia, O. D. *et al.* The role of alveolar epithelial cells in initiating and shaping pulmonary immune responses: communication between innate and adaptive immune systems. *PLoS one* **7**, e32125, <https://doi.org/10.1371/journal.pone.0032125> (2012).
28. Lloyd, C. M. & Marsland, B. J. Lung Homeostasis: Influence of Age, Microbes, and the Immune System. *Immunity* **46**, 549–561, <https://doi.org/10.1016/j.immuni.2017.04.005> (2017).
29. Fava, L. L., Bock, F. J., Geley, S. & Villunger, A. Caspase-2 at a glance. *J Cell Sci* **125**, 5911–5915, <https://doi.org/10.1242/jcs.115105> (2012).
30. Guo, Y., Srinivasula, S. M., Druilhe, A., Fernandes-Alnemri, T. & Alnemri, E. S. Caspase-2 induces apoptosis by releasing proapoptotic proteins from mitochondria. *J Biol Chem* **277**, 13430–13437, <https://doi.org/10.1074/jbc.M108029200> (2002).
31. Krumschnabel, G., Sohm, B., Bock, F., Manzl, C. & Villunger, A. The enigma of caspase-2: the laymen's view. *Cell Death Differ* **16**, 195–207, <https://doi.org/10.1038/cdd.2008.170> (2009).
32. Lopez-Cruzan, M. *et al.* Caspase-2 resides in the mitochondria and mediates apoptosis directly from the mitochondrial compartment. *Cell Death Discov* **2**, <https://doi.org/10.1038/cddiscovery.2016.5> (2016).
33. Wang, H. *et al.* Mixed lineage kinase domain-like protein MLKL causes necrotic membrane disruption upon phosphorylation by RIP3. *Molecular cell* **54**, 133–146 (2014).
34. Sakamaki, K., Imai, K., Tomii, K. & Miller, D. J. Evolutionary analyses of caspase-8 and its paralogs: Deep origins of the apoptotic signaling pathways. *Bioessays* **37**, 767–776, <https://doi.org/10.1002/bies.201500010> (2015).
35. Horn, S. *et al.* Caspase-10 Negatively Regulates Caspase-8-Mediated Cell Death, Switching the Response to CD95L in Favor of NF- κ B Activation and Cell Survival. *Cell Rep* **19**, 785–797, <https://doi.org/10.1016/j.celrep.2017.04.010> (2017).

36. Hagar, J. A., Powell, D. A., Achoui, Y., Ernst, R. K. & Miao, E. A. Cytoplasmic LPS activates caspase-11: implications in TLR4-independent endotoxic shock. *Science* **341**, 1250–1253, <https://doi.org/10.1126/science.1240988> (2013).
37. Binet, F., Chiasson, S. & Girard, D. Evidence that endoplasmic reticulum (ER) stress and caspase-4 activation occur in human neutrophils. *Biochem Biophys Res Commun* **391**, 18–23, <https://doi.org/10.1016/j.bbrc.2009.10.141> (2010).
38. Casson, C. N. *et al.* Human caspase-4 mediates noncanonical inflammasome activation against gram-negative bacterial pathogens. *Proc Natl Acad Sci USA* **112**, 6688–6693, <https://doi.org/10.1073/pnas.1421699112> (2015).
39. Krumschnabel, G., Manzl, C. & Villunger, A. Caspase-2: killer, savior and safeguard—emerging versatile roles for an ill-defined caspase. *Oncogene* **28**, 3093–3096, <https://doi.org/10.1038/onc.2009.173> (2009).
40. Susin, S. A. *et al.* Mitochondrial release of caspase-2 and -9 during the apoptotic process. *J Exp Med* **189**, 381–394 (1999).
41. Murphy, J. M. *et al.* The pseudokinase MLKL mediates necroptosis via a molecular switch mechanism. *Immunity* **39**, 443–453 (2013).
42. Gonzalez-Juarbe, N. *et al.* Requirement for *Serratia marcescens* cytolysin in a murine model of hemorrhagic pneumonia. *Infect Immun* **83**, 614–624, <https://doi.org/10.1128/IAI.01822-14> (2015).
43. Reyes, L. F. *et al.* Severe Pneumococcal Pneumonia Causes Acute Cardiac Toxicity and Subsequent Cardiac Remodeling. *Am J Respir Crit Care Med*, <https://doi.org/10.1164/rccm.201701-0104OC> (2017).
44. Reyes, L. F. *et al.* A Non-Human Primate Model of Severe Pneumococcal Pneumonia. *PLoS one* **11**, e0166092, <https://doi.org/10.1371/journal.pone.0166092> (2016).
45. Gilley, R. P. *et al.* Infiltrated Macrophages Die of Pneumolysin-Mediated Necroptosis following Pneumococcal Myocardial Invasion. *Infection and immunity* **84**, 1457–1469, <https://doi.org/10.1128/IAI.00007-16> (2016).

Acknowledgements

We thank Dr. Warren Alexander (Walter and Eliza Hall Institute of Medical Research Parkville, Victoria, Australia) for the gift of MLKL KO mice. N.G.-J. was supported by National Institutes for Health (NIH) Immunologic Diseases and Basic Immunology grant 5T32AI007051-38. M.I.R. was supported by Award Number K23HL096054 from the NHLBI. C.J.O. was supported by NIH grant A1114800 and American Heart Association grant 166RNT30230007. We thank Anukul T. Shenoy, and Ryan P. Gilley for technical support.

Author Contributions

N.G.-J., and C.J.O. wrote and edited the paper. N.G.-J. and C.J.O. designed the experiments. N.G.-J., A.N.R., L.F.R., T.B., M.I.R., S.S.P. and K.M.B. executed the experiments.

Additional Information

Supplementary information accompanies this paper at <https://doi.org/10.1038/s41598-018-24210-8>.

Competing Interests: The authors declare no competing interests.

Publisher's note: Springer Nature remains neutral with regard to jurisdictional claims in published maps and institutional affiliations.



Open Access This article is licensed under a Creative Commons Attribution 4.0 International License, which permits use, sharing, adaptation, distribution and reproduction in any medium or format, as long as you give appropriate credit to the original author(s) and the source, provide a link to the Creative Commons license, and indicate if changes were made. The images or other third party material in this article are included in the article's Creative Commons license, unless indicated otherwise in a credit line to the material. If material is not included in the article's Creative Commons license and your intended use is not permitted by statutory regulation or exceeds the permitted use, you will need to obtain permission directly from the copyright holder. To view a copy of this license, visit <http://creativecommons.org/licenses/by/4.0/>.

© The Author(s) 2018